DAΦNE TECHNICAL NOTE

INFN - LNF, Accelerator Division

Frascati, July 1, 2004

Note: **L-36**

PRELIMINARY RESULTS OF THE NONLINEAR BEAM DYNAMICS SIMULATION FOR THE STRONG RF FOCUSING RING (DAΦNE-II)

E. Levichev, P. Piminov

Budker Institute of Nuclear Physics, Novosibirsk 630090, Russia

1. Introduction

The main feature of a new project [1] is the large negative momentum compaction factor ($\alpha = -0.17$) and very high RF cavity voltage that provides the local (at the collision azimuth) bunch length compression. At the same time, the DAΦNE-II lattice [2] demonstrates significant natural chromaticity in vertical direction ($\xi_x \approx -5$, $\xi_z \approx -46$), which requires strong sextupole magnets for compensation. The following features of the DAΦNE -II nonlinear particle motion can be generally assumed:

(1) As the tune point is chosen close to the integer resonance ($Q_x \approx 8.14$), the horizontal 1D dynamic aperture has to be defined mainly by the resonance $Q_x = 8$ together with the third-integer resonance $3Q_x = 24$ that occurs at the same tune.

(2) However, it's not necessarily true for 2D motion because the integral strength of the sextupole magnets for vertical motion is much higher than that for the horizontal one. And even small initial vertical amplitude results in nonlinear coupling resonances and reduces the dynamic aperture.

(3) For 3D motion the synchro-betatron resonances play main part in reduction of energy dynamic aperture. Dispersion in the sextrupole magnets together with strong RF focusing provides dense web of satellite resonances close to the integer resonance line.

To check these assumptions and to study the dynamic aperture of the DAΦNE-II project, a simulation of the nonlinear beam dynamics was performed with the help of computer code ACCELERATICUM, which track particle in a 3D manner with the realistic path lengthening in all magnetic elements (it's important for correct simulation of the coupled synchro-betatron motion).

The lattice prepared by Caterina Biscari (epac04.mad) has the following general parameters listed in Table 1.

Table 1 – DAΦNE-II parameters.

E (MeV)	510
L (m)	114.24
α	-0.167
T_o (ns)	381
ξ_x, ξ_z	-5.6, -45.6
Q_x, Q_z	8.136, 8.144

All tracking results such as dynamic aperture or phase space plot refer to the collision point with the beam parameters reported in Table 2.

Table 2 – Lattice parameters at the output azimuth.

β_z^* (m)	$2\cdot10^{-3}$
β_x^* (m)	0.5
σ_z (m)	$1.5\cdot10^{-6}$
σ_x (m)	$4.0\cdot10^{-4}$
$\varepsilon_z / \varepsilon_x$	$3.6\cdot10^{-3}$
σ_e	$4.5\cdot10^{-4}$

2. On-energy dynamic aperture

For this tracking mode the energy oscillation was switched-off and the 2D simulation was performed. The following results are given in this note:

(a) nonlinear detuning coefficients according to the following notation:

$$\Delta Q_x = 2C_{11}J_x + C_{12}J_z, \qquad \Delta Q_z = C_{12}J_x + 2C_{22}J_z, \tag{1}$$

are given in Table 3.

Table 3 – DAΦNE-II nonlinear detuning coefficients.

C_{11} (m^{-1})	-26
C_{12} (m^{-1})	-130
C_{22} (m^{-1})	9

(b) values of the main sextupole resonances harmonics provides information about the most dangerous resonances in the vicinity of working point:

$$A_{1n} = \frac{1}{48\pi}\sum_m \beta_{xm}^{3/2}(k_2 l)_m \begin{matrix}\cos\\ \sin\end{matrix}(\psi_x - \nu\theta + n\theta)_m ,$$

$$A_{3n} = \frac{1}{48\pi}\sum_m \beta_{xm}^{3/2}(k_2 l)_m \begin{matrix}\cos\\ \sin\end{matrix}(3\psi_x - 3\nu\theta + n\theta)_m \tag{2}$$

$$B_{1n} = \frac{1}{48\pi}\sum_m \beta_{xm}^{1/2}\beta_{ym}(k_2 l)_m \begin{matrix}\cos\\ \sin\end{matrix}(\psi_x - \nu\theta + n\theta)_m$$

$$B_{\pm n} = \frac{1}{48\pi}\sum_m \beta_{xm}^{1/2}\beta_{ym}(k_2 l)_m \begin{matrix}\cos\\ \sin\end{matrix}(\psi_\pm - \nu_\pm\theta + n\theta)_m$$

Table 4 shows the strength of sextupole harmonics, which excite the resonances closest to the chosen tune point. The last column of the Table demonstrates the estimation of the driving term referring to the distance from the relevant resonance.

Table 4 – Parameters of the main sextupole resonances.

	n	C (m$^{-1/2}$)	S(m$^{-1/2}$)	δ	$\sqrt{C^2+S^2}/\delta$ (m$^{-1/2}$)
A_{1n}	8	-0.018	-0.007	$Q_x - n = 0.136$	0.14
A_{3n}	24	0.003	-0.058	$3Q_x - n = 0.41$	0.14
B_{1n}	8	0.080	0.024	$Q_x - n = 0.136$	0.62
B_{+n}	24	0.262	0.376	$Q_x + 2Q_z - n = 0.42$	1.09
B_{-n}	-8	-0.117	0.325	$Q_x - 2Q_z - n = 0.15$	2.31

(c) dynamic aperture

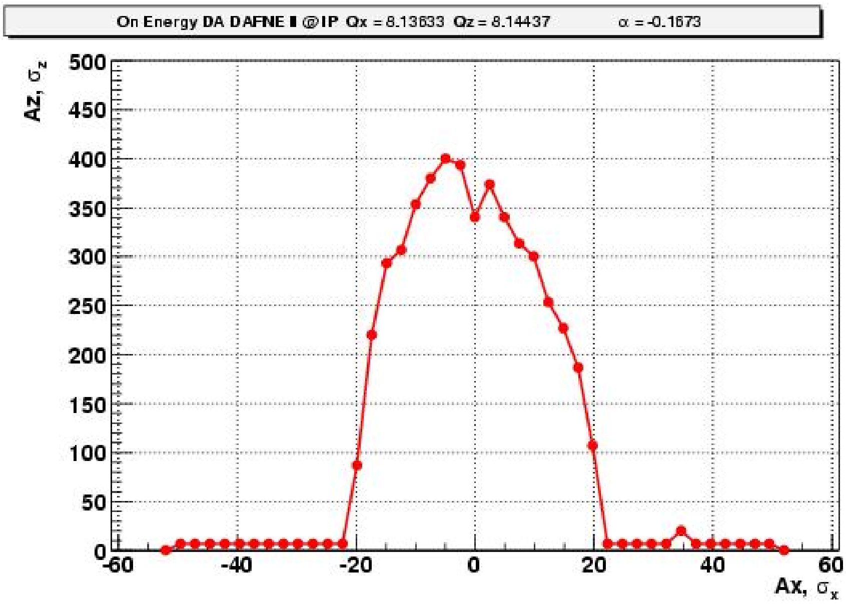

Figure 1 – The on-energy dynamic aperture. Note that the large horizontal DA shrinks when an arbitrary small vertical amplitude appears.

(d) phase trajectories

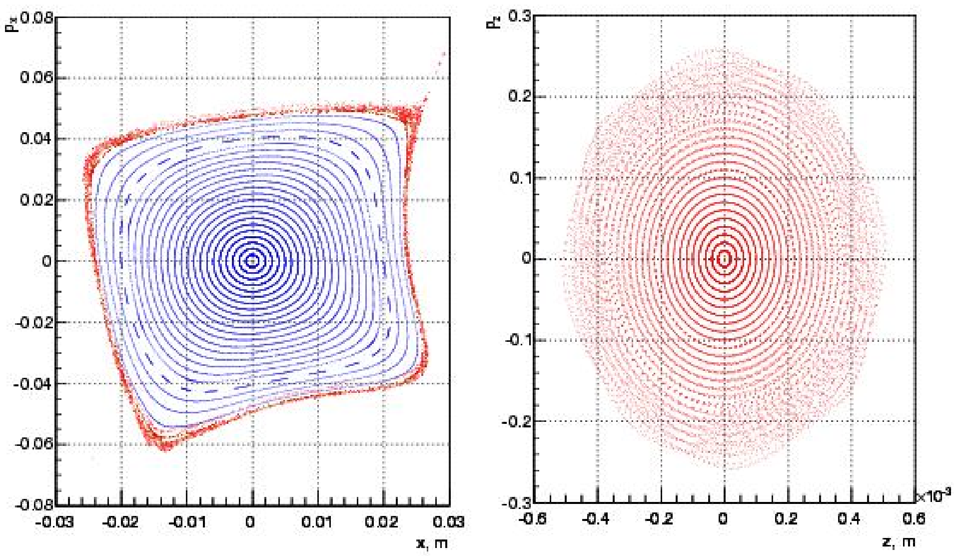

Figure 2 - The on-energy phase space portrait (horizontal and vertical).

Conclusion: for the 2D motion the sextupole coupling resonances (see C_{12}, B_{+n} and B_{-n}) strongly influence the beam behavior and determine the size of the stable motion area. To reduce this influence one can consider such arrangement of the chromatic sextupoles, which minimize the relevant harmonics (2).

3. Synchro-betatron motion

In the case under consideration, the only source of synchro-betatron resonances is the horizontal dispersion in sextupole magnets. For DA_NE-II with strong RF focusing the synchrotron tune is $Q_s \approx 0.4$ and in spite of this value is about two orders of magnitude larger than typical synchrotron tune, it is still much less than the betatron tune $Q_{x,z} \sim 8$ so we can use the formalism of A.Piwinski to estimate the effect.

According to [3], the following main satellite resonances are excited by the horizontal dispersion η_x in sextupole magnets:

Resonance	*Resonance width*
$2Q_x \pm Q_s = n$	$\Delta Q_x = \pm\hat{\delta}\left\lvert\sum_k \left[(ml)\cdot\eta_x\cdot\beta_x\cdot e^{2i\psi_x}\right]_k\right\rvert$
$2Q_z \pm Q_s = n$	$\Delta Q_z = \pm\hat{\delta}\left\lvert\sum_k \left[(ml)\cdot\eta_x\cdot\beta_z\cdot e^{2i\psi_z}\right]_k\right\rvert$
$Q_x \pm 2Q_s = n$	$\Delta Q_x = \pm\frac{\hat{\delta}^2}{2\sqrt{\varepsilon_x}}\left\lvert\sum_k \left[(ml)\cdot\eta_x^2\cdot\sqrt{\beta_x}\cdot e^{i\psi_x}\right]_k\right\rvert$

where $\hat{\delta}$ is the synchrotron oscillation amplitude: $\delta = \delta\cdot\cos Q_s\theta$, $\varepsilon_x = A_x^2/\beta_x^*$ and the sum is taken over sextupole magnets with integrated strength $(ml)_k$. Note that only the rise times (inversely proportional to the resonance width) on $2Q_{x,z} \pm Q_s = n$ give an exponential increase. The rise time for $Q_x \pm 2Q_s = n$ depend on the horizontal amplitude and change with its increasing.

The value of the synchro-betatron lattice factors was calculated to understand, which satellite is more dangerous for the motion (Table 5).

Table 5 – Synchro-betatron satellites lattice factor.

$2Q_x \pm Q_s = n$	62
$2Q_z \pm Q_s = n$	68
$Q_x \pm 2Q_s = n$	0.2

For the first two resonances the absolute value of corresponding sums are given in Table 5 while for the last one the sum is multiplied by the factor $\hat{\delta}/\sqrt{\varepsilon_x} \approx 0.1$, which corresponds approximately to the middle of stable area. All these satellites can be compensated by varying the sextupole strength so that the lattice factors for main resonances vanish.

If the fractional tunes of betatron and synchrotron oscillation are comparable, a density of resonance line at the tune diagram increases drastically. For our case the satellite resonance lines are plot in Fig. 3.

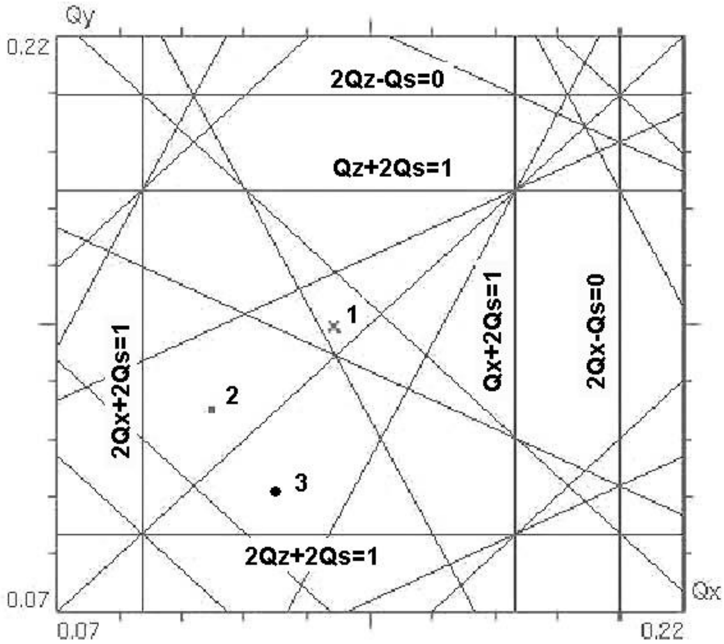

Figure 3 - Tune diagram (only the synchro-betatron satellite lines are shown).
Three tune points are: 1 ($Q_x = 8.136, Q_z = 8.144$), 2 ($Q_x = 8.107, Q_z = 8.121$) and 3($Q_x = 8.120,\ Q_z = 8.102$).

A 3D tracking was performed for 10 MV peak RF voltage and 472 MHz RF frequency (harmonic number is 180). The 2D and 3D betatron oscillation spectrum (for small initial betatron amplitudes) are shown in Fig.4. An excitation of the satellite lines is clearly seen at this plot.

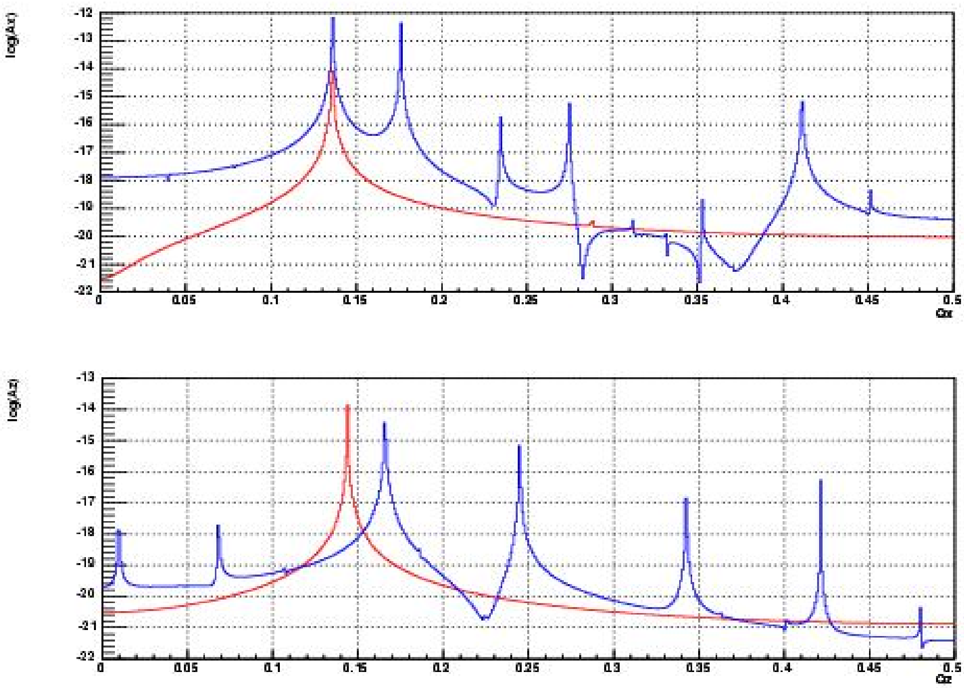

Figure 4 - 3D motion spectrum (blue line) and 2D motion spectrum (red line).

Several betatron tune points were explored in order to optimize the momentum dynamic aperture. At the initial point ($Q_x = 8.136, Q_z = 8.144$) the vertical dynamic aperture drops down very fast with increasing of the synchrotron oscillation amplitude (Fig. 5), so the maximum energy aperture is less than $5\sigma_e$ and can not provide good beam lifetime.

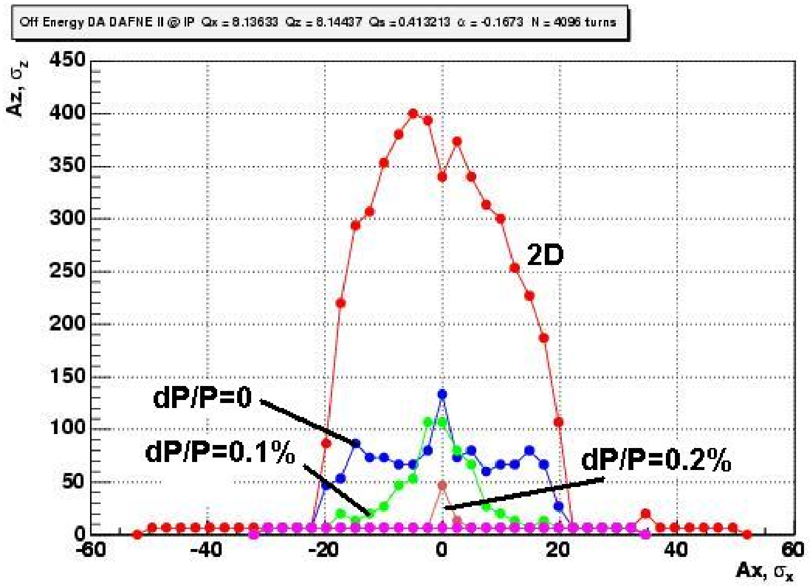

Figure 5 - A 3D dynamic aperture for $Q_x = 8.136$ and $Q_z = 8.144$.

Note also that the on-energy aperture in Fig. 5 is rather large, however when the 3D mode is switched on, the vertical aperture reduces drastically even for $\delta = 0$. The reason is the large momentum compaction factor and hence the large path lengthening due to the betatron oscillation.

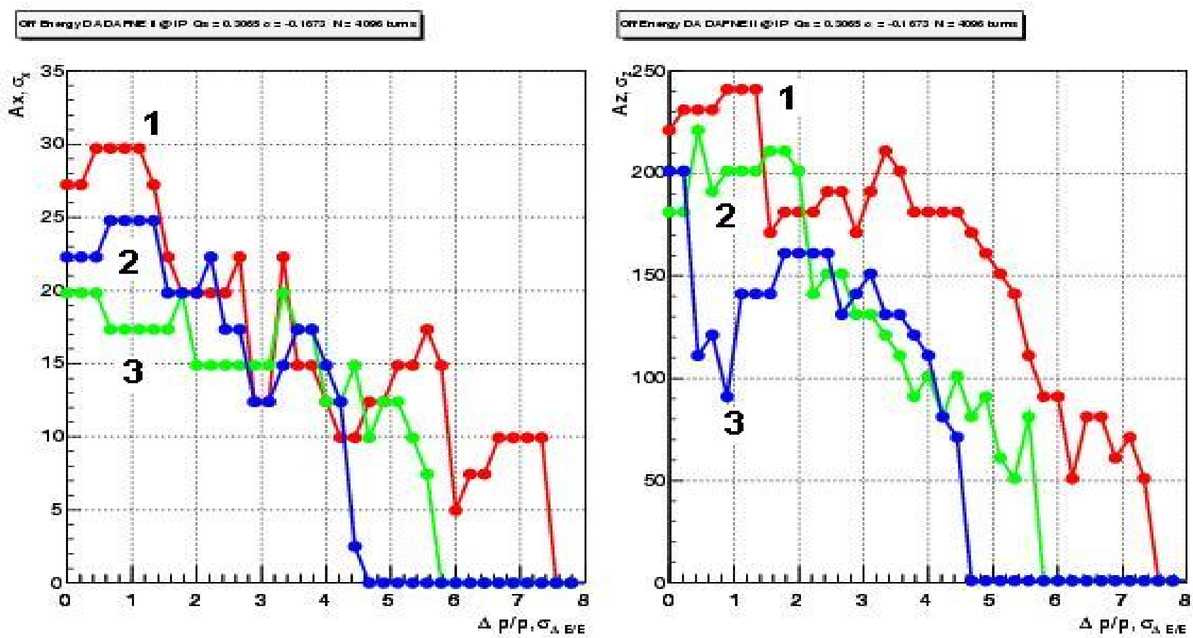

Figure 8 - Horizontal and vertical dynamic aperture as a function of the synchrotron oscillation amplitude for 3 tune points.

4. Conclusion

Nonlinear beam motion of particle in the DAΦNE-II storage ring was studied numerically in presence of chromatic sextupoles and the betatron tune point was selected to provide reasonable dynamic aperture as a function of energy deviation. The 2D dynamics displays strong influence of sextupole coupling while the 3D simulation shows an importance of synchro-betatron resonances as an essential factor of the energy aperture limitation.

Further investigation of this machine with strong RF focusing and large negative momentum compaction factor may include the following items:

1. Optimization of the chromatic sextupoles scheme to reduce the harmonics responsible for the sextupole coupling resonances.
2. Optimization of the lattice factors driving the synchro-betatron satellite resonances. Further study (tune scan) of the synchro-betatron resonances including nonlinear ones would be valuable.
3. Other sources of the synchro-betatron coupling including spurious vertical dispersion in the sextupole magnets, small dispersion error in the RF cavity (very high voltage), path lengthening (large alpha), beam-beam effects, etc. have to be carefully considered.

5. References

[1] A. Gallo, P.Rimondi, M.Zobov "Strong RF focusing for luminosity increase", e-Print Archive: physics/0309066.
[2] Caterina Biscari, DAΦNE-II magnetic lattice, EPAC04.mad (June, 2004).
[3] A. Piwinski, Synchrotron Sidebands of Betatron Coupling Resonances", DESY 93-189 (1993).
[4] A. Piwinski, A.Wrulich, DESY 76/07 (1976).